

Analysis of smectic structure formation in liquid crystalline thermosets

Atsushi Shiota* and Christopher K. Ober†

Department of Materials Science and Engineering, Bard Hall, Cornell University, Ithaca, NY 14853-1501, USA

(Received 14 October 1996; revised 27 January 1997)

Smectic network formation using a twin liquid crystalline epoxy monomer (4-(oxiranymethoxy)benzoic acid 1,8-octanediylbis(oxy-4,1-phenylene) ester) cross-linked with sulfanilamide was examined in real time by polarizing optical microscopy, X-ray diffraction, dynamic viscometry and differential scanning calorimetry. The initial curing reaction of the twin epoxy monomer and sulfanilamide was found to be diffusion controlled because of the heterogeneity of the system. An acceleration of the curing rate was observed a critical time after the start of the reaction. It was found that the adduct of the twin epoxy monomer and sulfanilamide produced a smectic phase even though the twin epoxy monomer itself only displayed a nematic phase. The strong interaction of the sulfonamide function may contribute to the formation of smectic order. A change in curing behaviour took place when the curing reaction was carried out above $\sim 170^\circ\text{C}$. Above this transition region, a smectic phase forms directly from an isotropic melt. On the other hand, below this transition, the smectic phase forms via a transient nematic phase. Cross-linking causes fine disclination lines in the optical texture as well as a decrease of the smectic layer spacing. © 1997 Elsevier Science Ltd.

(Keywords: thermoset; liquid crystal; smectic)

INTRODUCTION

The construction of densely cross-linked networks from liquid crystalline (LC) monomers is being studied as a means of preparing new materials with unusual mechanical and optical properties^{1,2}. In addition to these goals, LC thermosets offer the possibility of producing bulk layered structures with macroscopic orientation if cured in an aligning field. Such new materials provide interesting possibilities as separation or transport media as well as being large dimension analogues to Langmuir–Blodgett films provided that smectic-like order can be formed in the network.

Several approaches in particular to the construction of densely cross-linked smectic networks have been reported. Previous studies of smectic networks required a low curing rate to form smectic order. For example, in the case of LC epoxy networks, a smectic network was only obtained when a reactant mixture of LC epoxy monomer and hardener were cured in a nematic phase just above the eutectic temperature^{3,4}. The reactant mixture when processed at a higher temperature usually forms a nematic network. Alternatively, when a mesogenic epoxy compound was reacted with a curing agent having two groups with unequal reactivities such as sulfanilamide (SAA), a smectic-like structure resulted^{5,6}. These ‘dual-reactivity’ curing agents allow a wider processing flexibility than the former method. However, the high melting point of SAA at 165°C and its low

reactivity is one of the disadvantages of this curing agent. It is also possible to design an LC monomer especially for smectic network formation. In our previous paper, we demonstrated preferential formation of smectic networks from thermoset monomers having an LC twin architecture (twin LC epoxy monomer)⁷. It appeared that network formation induced registration between the mesogenic groups that was absent in the unpolymerized melt and transformed the LC organization from nematic to smectic.

One of the aims of our studies has been to understand how the smectic structure forms from the two different components in an LC epoxide–diamine system. For this purpose, we chose a combination of a twin LC epoxy monomer and SAA. 4-(Oxiranymethoxy)benzoic acid 1,8-octanediylbis(oxy-4,1-phenylene) ester (CAS registry number: 173844-51-4), which we call Twin8e shows a nematic phase above the melting point at 152°C , a temperature which is close to the melting point of SAA (165°C) (Figure 1). In a previous paper, we reported that this combination formed a smectic-like network when cured between 160 and 200°C . SAA provides a moderate curing rate over this temperature range because of its low reactivity, allowing for various real-time measurements to be carried out. Combining and comparing various characterization methods is necessary to understand how both the state of order and the curing reaction are affected by each other. Isothermal and dynamic experiments with d.s.c., viscometric measurements, cross-polarizing optical microscopy (POM) observations and real-time X-ray diffraction measurements were employed to analyse smectic structure formation.

* Present address: Japan Synthetic Rubber Co., Ltd, Tsukuba Research Laboratory, 25 Miyukigaoka, Tsukuba-Shi, Ibaraki, 305 Japan

† To whom correspondence should be addressed

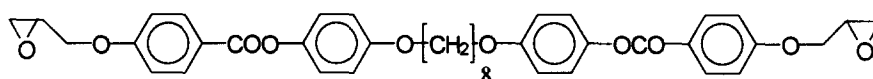


Figure 1 Structure of the twin LC epoxy monomer Twin8e

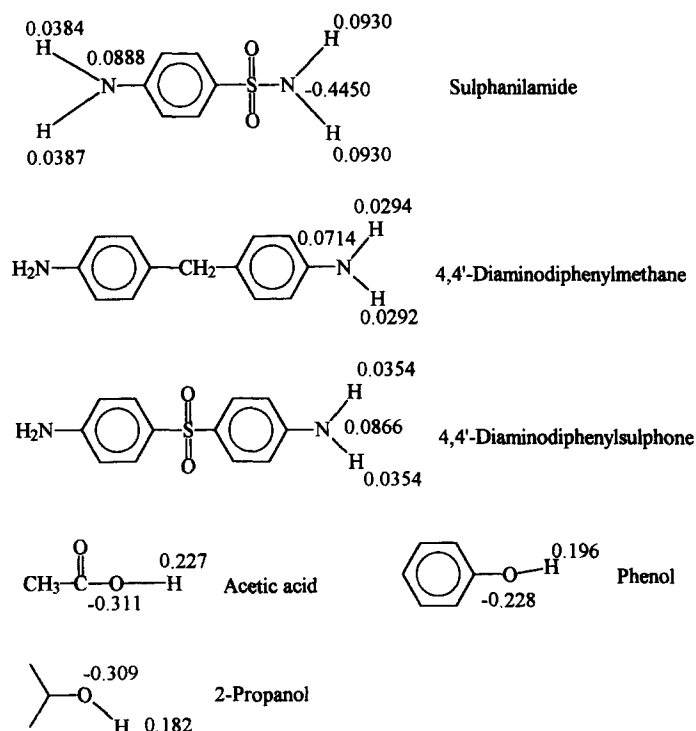


Figure 2 Mulliken electron charge distribution for various epoxy resin curing agents

EXPERIMENTAL

The synthesis and purification of the twin LC epoxy compound Twin8e has been described previously⁷. SAA purchased from the Aldrich Chemical Co. was used without further purification. Stoichiometric amounts of the diepoxy monomer (2 mol) and SAA (1 mol) were ground in a mortar and pestle to produce the reactant mixture.

A DuPont 910 differential scanning calorimeter was used both for isothermal and dynamic experiments. The dynamic d.s.c. study was carried out with a heating rate of 20°C min⁻¹. For the isothermal measurement, a sealed aluminium sample pan was inserted into the differential scanning calorimeter cell equilibrated at the required temperature as quickly as possible. After the isothermal experiment, a baseline signal was obtained with the same fully cured sample to compensate for an initial off-balance signal. Finally, an isothermal heat flow curve was corrected to subtract the baseline signal from the exothermic signal of the reaction, assuming that the difference in heat capacity before and after reaction is negligible.

Mesophases were examined using a Nikon polarizing optical microscope (OPTIPHOT2-POL) at 100× and 200× magnification equipped with a Mettler FP-82HF hotstage and a photomonitor.

Real-time X-ray diffraction data were obtained at the Cornell High Energy Synchrotron Source (CHESS) facilities at Cornell University. The sample temperature was regulated using a Mettler FP-82HF Hotstage mounted in the beam path. Flux of a monochromated beam of 0.910 Å wavelength counted at 27000 cps

(0.3 mm diameter collimator) allowed exposure times of less than 1 s. X-ray diffraction images were recorded on a charge-coupled device detector every 30–40 s, including data transfer and processing time, and were finally saved as 16-bit resolution Tiff format files.

Viscometric measurements were performed with the aid of a Rheometrics RDA-II dynamic mechanical spectrometer using 25 mm diameter parallel-plates geometry. A pressed sample cake (20 mm diameter) was inserted in the preheated spectrometer, and the measurement started with a shear rate of 10 rad s⁻¹ and 1% of strain.

Mulliken's electron charge densities of compounds used in this study were calculated using MOPAC Ver. 6.12⁸. Keywords of PM3, SYMMETRY, DENSITY and XYZ were selected for the calculation.

RESULTS AND DISCUSSION

Reactivity of SAA

SAA is an aromatic diamine with two different amine functions. When a rigid-rod epoxy compound is reacted with a curing agent such as SAA with amine groups of unequal reactivities, a smectic-like structure results. The smectic-like structure has been confirmed by both polarizing optical microscopy by Lin *et al.*⁵ and by X-ray diffraction experiments in our research group⁶. Lin *et al.* claimed that these 'dual-reactive' curing agents allow sufficient chain extension before cross-linking occurs. They explained that the more reactive group of the 'dual-reactivity' curing agent behaves as a chain

extension agent while the group with lower reactivity subsequently completes the cross-linking reaction.

While this interesting property of SAA has been previously reported, reaction kinetics between the epoxy function and SAA have not been examined in detail. SAA is much less reactive than other aromatic amine compounds, as electrons on the nitrogen atom in the amine function are strongly withdrawn by the sulfone function. Figure 2 shows Mulliken's electron density populations for several model epoxy resin hardeners calculated using the PM3 method. The results show that the more positively charged nitrogen atom on the amine function of SAA is less nucleophilic than that of diaminodiphenylmethane. This means that the basicity of the amine is quite low. The reactivity of the amine function of SAA is therefore expected to be close to that of 4,4-diaminodiphenylsulfone (DDS), based on the results of a molecular orbital calculation. In fact, because the nitrogen atom on the SAA amide group is negatively charged, hydrogen atoms attached at the nitrogen

become acidic. The hydrogen atom on the sulfonamide group presumably acts as a weak acid similar to phenol or a carboxylic acid. Thus, the two reactive groups on SAA have opposite and unequal reactivities much like a weak base and weak acid.

In order to investigate the kinetics of the reaction between SAA and an epoxy function, isothermal cure experiments using d.s.c. were carried out with stoichiometric mixtures of 2,2'-[(1-methylethylidene)bis(4,1-phenyleneoxymethylene)]bisoxirane (DGEBA) and SAA over a 160–190°C temperature range up to 180 min. D.s.c. is commonly used to determine rates of reaction and degree of cure under the assumption that heat flow relative to the instrumental baseline is proportional to reaction rate^{9,10}. If it is assumed that molecules react by a constant heat of reaction per molecule, then fractional conversion α is described with the partial heat of reaction Q_t and the overall heat of reaction Q_0 given by

$$Q_0 = \int_0^{\infty} \left(\frac{dq}{dt} \right) dt \quad (1)$$

$$Q_t = \int_0^t \left(\frac{dq}{dt} \right) dt \quad (2)$$

$$\alpha = \frac{Q_t}{Q_0} \quad (3)$$

$$\frac{d\alpha}{dt} = \left(\frac{dq}{dt} \right) Q_0^{-1} \quad (4)$$

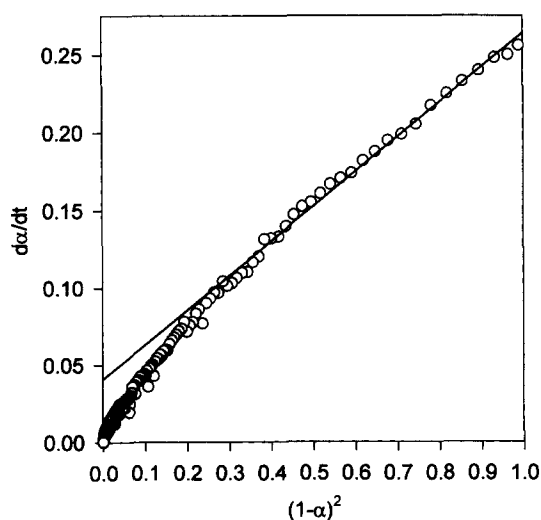


Figure 3 Second-order kinetic analysis for isothermal curing reaction of DGEBA/SAA at 175°C

where q is the heat flow detected by d.s.c. Figure 3 displays results of the isothermal cure experiment at 175°C of a stoichiometric mixture of the DGEBA and SAA. This result shows that the kinetics of the reaction between the DGEBA and SAA can be described as a simple second-order reaction over a wide range of monomer concentration because the rate of cure ($d\alpha/dt$) is proportional to $(1-\alpha)^2$, which expresses the monomer concentration. The same trends were noted over a 160–190°C temperature range. Then, the activation energy of 75.7 kJ (epoxy equivalent)⁻¹ was calculated

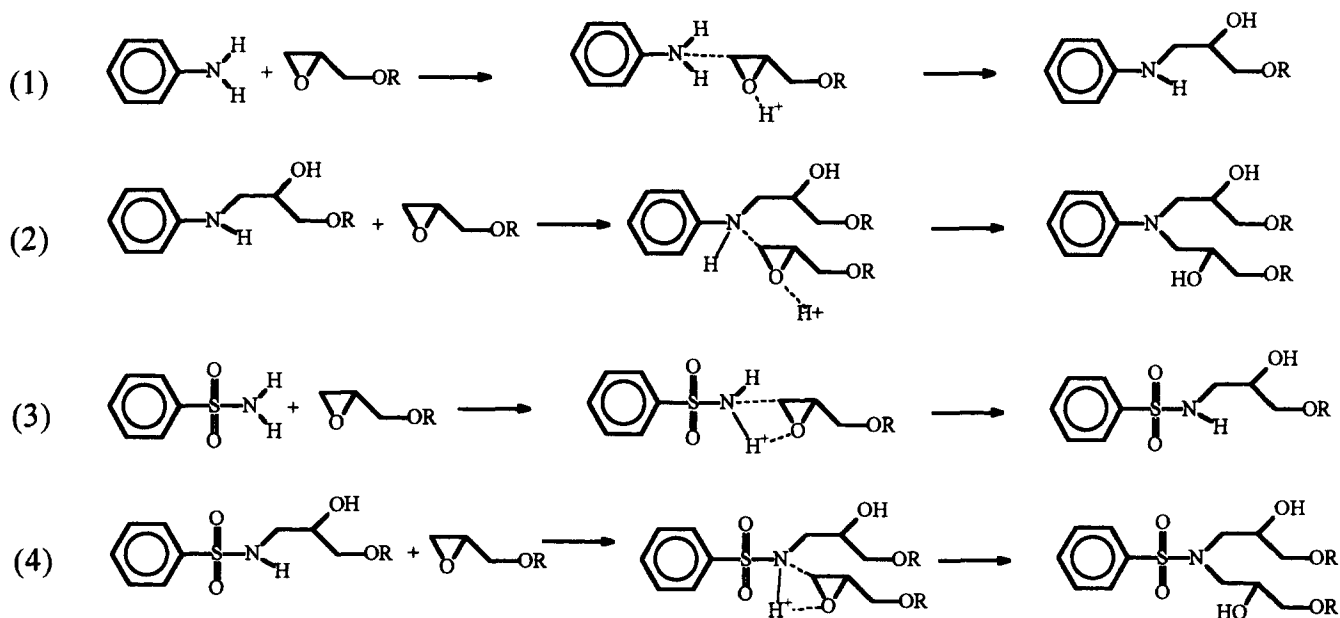


Figure 4 Four possible pathways in the reaction between SAA and an epoxy function

from the rate constants at conversions less than $\alpha = 0.55$. The total heat of reaction was -86.3 ± 2.8 kJ (epoxy equivalent) $^{-1}$ and approximately constant over the examined temperature range (160–190°C).

An initial acceleration of the reaction rate catalysed by hydroxy groups produced during curing is commonly observed in various combinations of epoxy monomers and amine compounds. However, no apparent autocatalytic behaviour was observed for the DGEBA/SAA combination used in this study. This observation may be mainly due to the slightly acidic hydrogen atoms on the amide function of SAA which act as catalytic proton donors for reactions between the amine function of SAA and the epoxy group. Lin *et al.* reported that the amine function of SAA is more reactive than the amide function of SAA¹¹. The reaction mechanism, therefore, can be described by four different reaction steps as illustrated in Figure 4, which are: (1) reaction between the SAA primary amine and an epoxide, (2) reaction between the secondary amine of the SAA amine function and an epoxide, (3) reaction between the primary amine of the SAA amide function and an epoxide, and (4) reaction between the secondary amine of the SAA amide function and an epoxide. Each of the reactions will have a different rate constant, because the reaction rate between a primary aromatic amine and an epoxide is generally twice or even more than that for a secondary amine due to steric hindrance on the secondary amine⁹. The curing reaction between SAA and epoxy functions should therefore be more complex, even though the experimental data can be fitted to a simple second-order kinetic equation.

One possible explanation for the apparent simplicity of the overall reaction kinetics involves the hydrogen atom of the secondary alcohol, which is generated by reaction (1) and is more acidic than the sulfonamide function of SAA. The rate constants of reactions (1) and (2) become identical, with the result that the hydroxy proton reduced the activation energy for reaction (2). Similarly, the tertiary amines generated by reaction (2) reduced the activation energy of reactions (3) and (4). In addition, as the hydrogen atom on the secondary amide

is more acidic than that on the primary amide, reduction of the rate constant by steric hindrance may be small.

As a result of these effects, only a small increase in rate constant was observed at a fractional conversion of $\alpha = 0.55$. This behaviour is in contrast to a conventional epoxy and amine reaction in a similar region of α where rate reduction occurs due to gelation. Even though the reaction mechanism is complicated, the evident simplicity of the reaction is very useful for examining the complex relationship between cross-linking and self-assembly in LC thermosets.

Isothermal POM studies of the Twin8e/SAA curing reaction

Evolution of the mesophase during the Twin8e/SAA curing reaction under isothermal conditions was observed using POM. In order to monitor growth of the LC state, the microscope was equipped with a photomonitor, and light intensity from birefringence was recorded on a personal computer. Observed light intensity was normalized relative to the light intensity of the nematic phase of Twin8e at 160°C. Figure 5 shows results of the POM experiments at several temperatures. Over the examined temperature range (160–190°C), the evolution of the mesophase during the curing reaction can be characterized by four critical regions:

Regime I. The reactant mixture showed no birefringence.

Regime II. Birefringent droplets emerged in the isotropic melt at time t_{m1} , and the number of droplets increased upon curing. This caused a continuous increase of the relative birefringent light intensity.

Regime III. At time t_{m2} , the relative light intensity showed a maximum value (I_{m2}) when the entire viewing area became birefringent, followed by an increasing disclination structure which reduced the birefringence.

Regime IV. At time t_{m3} , the structure is locked into a network at which point the formation of disclination lines stopped, and the light intensity saturated at value (I_{m3}).

Curing of the Twin8e/SAA system above 180°C followed a slightly different response. No maximum in the light intensity (t_{m2}) was observed. Even in regime II, disclination lines were observed. Table 1 shows the values of t_{m1} , t_{m2} , and t_{m3} , observed under various curing temperatures.

The relative light intensity was observed not only as a function of reaction time but also as a function of the

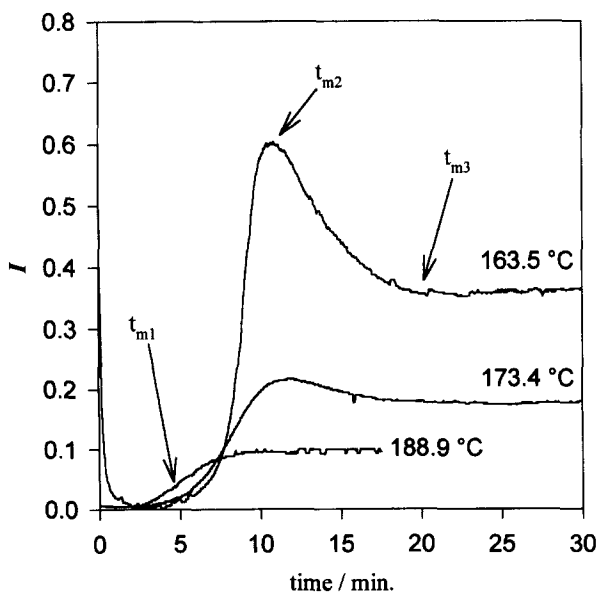


Figure 5 Evolution of the birefringence observed as changes in light scattering intensity (I) through crossed polarizers upon isothermal curing of the Twin8e/SAA system at 163.5, 173.4 and 188.9°C

Table 1 Times of transition observed with a cross-polarizing optical microscope, the Twin8e/SAA system at various cure temperatures

Cure temperature (°C)	t_{m1} (min)	t_{m2} (min)	t_{m3} (min)
164	3.33	11.0	19.0
166	3.33	12.5	18.6
169	3.69	12.6	17.9
171	4.17	12.5	16.6
173	4.00	11.8	15.0
176	2.60	10.0	13.9
179	2.61	9.3	10.5
184	2.14	—	9.0
189	3.21	—	8.5

t_{m1} : time when birefringence appeared

t_{m2} : time when birefringence reached the maximum intensity

t_{m3} : time when birefringence saturated

curing temperature (see Figure 6). As the processing temperature was raised, the value of the saturated light intensity (I_{m3}) tended to decrease due to disclination formation. The fractional conversion between 0.50 and 0.55 where disclination lines appeared was close to the theoretical gel point for a stoichiometric mixture. An increase in the difference between I_{m2} and I_{m3} was observed below the curing temperature of 168°C, indicating that fewer disclinations were formed at low cure temperature. Curing above 180°C did not produce a maximum in birefringent intensity.

There was an intermediate regime between 168 and 180°C in which only a small decrease in intensity was observed after reaching a maximum value. The thermal motion of reaction sites favours the formation of disordered networks even though both anisotropic dispersion and steric packing interactions work to restore the mesophase. It is only natural, therefore, for an LC thermoset that curing at high temperature produces a more disclination-rich structure due to a reduction of LC order. The relationship between the formation of disclination lines, the phase transition and the extent of the cross-linking reaction will be discussed later in the context of results from isothermal d.s.c. experiments and isothermal real-time X-ray diffraction measurements.

Isothermal d.s.c. studies of the curing of Twin8e/SAA

One of the purposes of this research was to observe how chemical structure affects the evolution of the mesophase. Results from POM experiments suggest that chemical structure plays an important role in stabilizing the LC state. It is possible to imagine several possible structures along the reaction pathway for the curing of an epoxy system with an amine. For this purpose, isothermal curing experiments using d.s.c. were carried out over a 160–190°C temperature range in the same manner as the DGEBA/SAA mixture. The extent of the polymerization (fractional conversion) as a function of time was calculated from an integration of the heat flow.

Figure 7 shows changes in rate of conversion *versus*

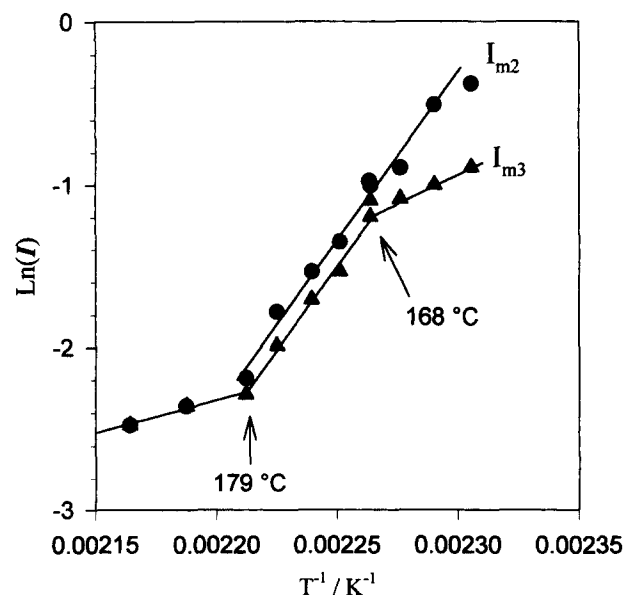


Figure 6 The relationship between cure temperatures and light scattering intensity (I) from birefringence. I_{m2} is the maximum intensity from birefringence. I_{m3} is the intensity at the saturated point

reaction time for the Twin8e/SAA reaction under several isothermal conditions. An exothermic peak appeared after an initial drop in the heat of reaction. This phenomenon occurs in marked contrast to the reaction of the DGEBA/SAA mixture, which shows only simple exponential decay of the heat of reaction. In the initial regime, it is thought that the reaction of Twin8e/SAA proceeded via a second-order kinetic reaction as did the DGEBA/SAA mixture. However, after some curing, the Twin8e/SAA reaction accelerated rapidly. This increased rate cannot be explained by an autocatalytic mechanism caused by generation of hydroxy groups. Enhancement of reaction rate in an LC state has been reported in both an acrylic system¹² and in a bisacetylene system¹³. However, in our system, it is premature to conclude that the accelerated rate was due only to a higher mesophase-induced reaction rate. The starting mixture of Twin8e/SAA is microscopically heterogeneous, while reactions of the LC acrylic system and the bisacetylene system start from a homogeneous state. In addition, as shown by the POM results, the system displayed an isotropic-LC biphasic for an extended period (5–7 min) before the entire area formed a mesophase. For the Twin8e/SAA system, both methods of either melt mixing or solution mixing are inadequate for uniform phase production, since Twin8e has poor solubility in common

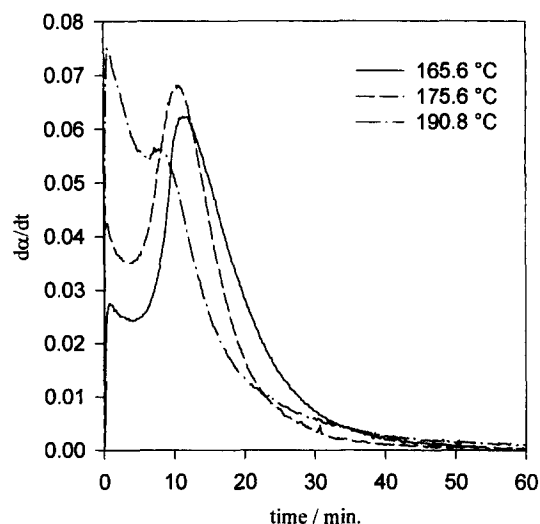


Figure 7 Rate of conversion ($d\alpha/dt$) as a function of reaction time at isothermal temperatures of 165.6, 175.6 and 190.8°C for the Twin8e/SAA system

Table 2 Results of isothermal d.s.c. studies for the stoichiometric mixture of the Twin 8e/SAA system

Cure temperature (°C)	t_{d1} (min)	α_{d1} (%)	t_{d2} (min)	α_{d2} (%)	ΔH (kJ(epoxy equivalent) ⁻¹)
165.5	2.16	0.054	12.28	0.473	-84.8
170.6	2.47	0.075	12.09	0.521	-87.3
175.6	2.15	0.083	11.49	0.535	-88.5
180.7	2.07	0.097	10.87	0.551	-87.5
186.1	2.48	0.136	10.50	0.543	-89.9
190.8	3.12	0.205	9.14	0.540	-86.8

t_{d1} : time when an acceleration of reaction started. α_{d1} : corresponding fractional conversion to t_{d1}

t_{d2} : time when an acceleration of reaction reached its peak. α_{d2} : corresponding fractional conversion to t_{d2}

ΔH : total heat of reaction per epoxy equivalent

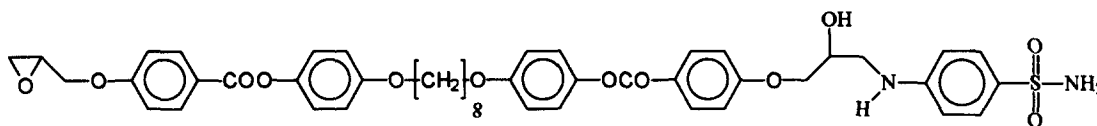


Figure 8 Structure of the Twin8e-SAA adduct

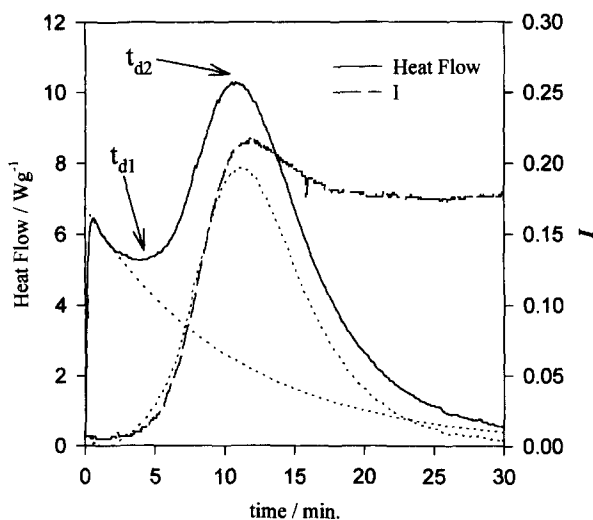


Figure 9 Comparison of evolution of birefringence (broken line) and d.s.c. trace (solid line) at the same isothermal cure temperature of 174°C for the Twin8e/SAA system. Two dotted lines indicate an exponential decay portion and the accelerated portion of the d.s.c. trace

organic solvents and both Twin8e and SAA have relatively high melting points. Isothermal d.s.c. experiments showed nearly identical mixing results for samples which were prepared by either the solvent-mixing method or by the simple mortar-mixing method.

We consider that the presence of microscopic heterogeneity may cause an acceleration of the reaction rate. The initial decay rate of the apparent second-order reaction of Twin8e/SAA was one-third to one-sixth times slower than that of DGEBA/SAA; nevertheless, an activation energy of 56.3 kJ (epoxy equivalent)⁻¹ for the Twin8e/SAA was lower than the activation energy of 75.7 kJ (epoxy equivalent)⁻¹ for the DGEBA/SAA. This fact indicates that the reaction of Twin8e/SAA at the initial stage of curing was already diffusion controlled.

As the system became homogeneous, the reaction rate increased. The acceleration of reaction rate stopped when the fractional conversion (α) reached a value of ~ 0.5 , when most of the monomers were converted to the Twin8e-SAA adducts or larger products (Table 2 and Figure 8). This phenomenon cannot be attributed to either gelation or the unequal reactivity of amine functions in SAA because, as we mentioned, the rate of reaction showed a small increase above $\alpha = 0.55$ in the case of the DGEBA/SAA system. The results of the POM experiments agreed well with the results of the isothermal d.s.c. experiments over the 165–190°C temperature range. The time where the onset of the mesophase occurred was close to the time (t_{d1}) where acceleration of reaction rate started. The time when the entire sample formed a mesophase corresponded to the time (t_{d2}) where the exothermic heat flow reached its peak (Figure 9).

Similar results to the Twin8e/SAA system were reported for the diglycidyl ether of 4,4'-dihydroxy- α -methylstilbene (DOMS) and 1,6-diaminotoluene (DAT) system by Amendola *et al.*¹⁴, and a 4,4-bis(oxyranlyl-

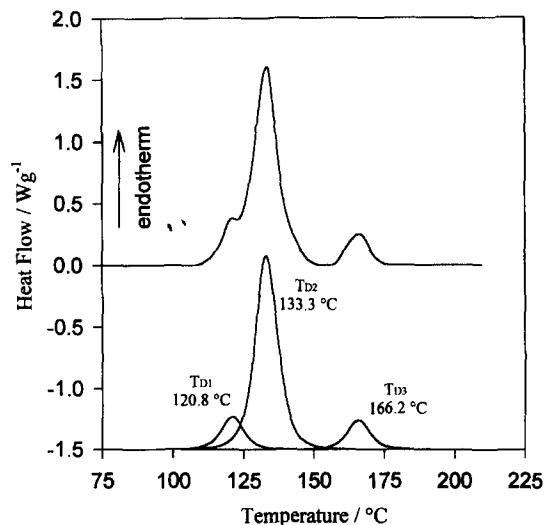


Figure 10 A dynamic d.s.c. trace of the Twin8e/SAA system cured at 175°C for 3 min. Fractional conversion of the sample was approximately 0.10

methoxy)biphenyl-diamine system by Mormann *et al.*¹⁵. The isothermal d.s.c. scans showed two exothermic peaks. Amendola *et al.* claims that the second exothermic peak can be ascribed to a high reaction rate in the nematic phase. In contrast, Mormann *et al.* reported that a system which is heterogeneous during the reaction showed two exothermic peaks while a system which is homogeneous displayed no second exothermic peak. We believe that miscibility of both the monomer and oligomer is one of the dominant factors for both reaction kinetics and formation of a mesophase in a multicomponent LC thermoset such as an LC epoxy-diamine system.

Real-time d.s.c. and POM studies of the Twin8e/SAA curing reaction

Studies of curing made with d.s.c. were likewise carried out in order to obtain transition temperatures of the intermediates. The dynamic d.s.c. studies of Twin8e/SAA were conducted as follows. Stoichiometric mixtures of Twin8e/SAA were placed in a series of sealed aluminium d.s.c. pans, and then cured in a hotstage of 165, 175 and 180°C for varying lengths of time. The pans were removed from the hotstage and subjected to d.s.c. scans from 25 to 230°C at a heating rate of 20°C min⁻¹. Figure 10 shows a typical d.s.c. trace of the Twin8e/SAA intermediate. The results suggest that a mesophase exists between ~ 130 and ~ 170 °C for the intermediate stage of the curing reaction. Also, the lower endothermic transition consists of two peaks. One small peak is located around 120°C (T_{D1}) and the other large peak is located around 133°C (T_{D2}). Figure 11 shows that a non-equilibrium phase diagram may be constructed from these d.s.c. data using both the lower (T_{D2}) and the upper transition (T_{D3}). The cure time was converted to fractional conversion from the corresponding isothermal d.s.c. results in order to normalize the data obtained

under different cure temperatures. As the figure shows, the data obtained at three different temperatures may be plotted on the same curves. This means that the intermediate compositions given under the different temperatures were identical for a given extent of polymerization. The phase diagram shows that as the reaction proceeded, the mesophase temperature range of the Twin8e/SAA system expanded. Douglas *et al.*¹³ reported a similar result for bisacetylene thermosets. They claimed that chain extension of a linear oligomer favoured an increase in the stability of the LC state. However, in our case, expansion of the mesomorphic region occurred up to a fractional conversion of 0.3. Also, as shown in Figure 12, enthalpies for T_{D3} continued to decrease as the reaction took place. If an oligomer did function to stabilize the mesophase, an increase in enthalpy, not a decrease, should be observed before gelation occurred. The maximum value of the enthalpy occurred at a conversion of only 0.10–0.15, then decayed. Furthermore, the Twin8e/SAA mixture was heterogeneous, in contrast to the bisacetylene system.

However, this hypothesis contradicts results of the isothermal POM experiments, where the mesophase continued to increase up to a conversion of 0.5, and mesophases were observed when the Twin8e/SAA system was processed above the upper transition point (T_{D3}). POM experiments corresponding to the dynamic d.s.c. measurements resolved these contradictions. A sample having a fractional conversion of 0.1–0.2 prepared in the same manner as the dynamic d.s.c. experiments was subjected to POM. Then, the temperature was scanned from 25 to 220°C at the same heating rate of 20°C min⁻¹. During the scan, the optical texture was observed. Simultaneously the intensity of scattered light from birefringence was recorded. Figure 13 shows recorded changes of light intensity. The same transitions which were obtained by d.s.c. measurements were observed at around 127 and 178°C. The lower temperature transition was a melting point. Above the melting point, a Schlieren texture was observed, while at the same time, a small amount of Batônnet texture was observed. Around 165°C, the Schlieren texture began to turn

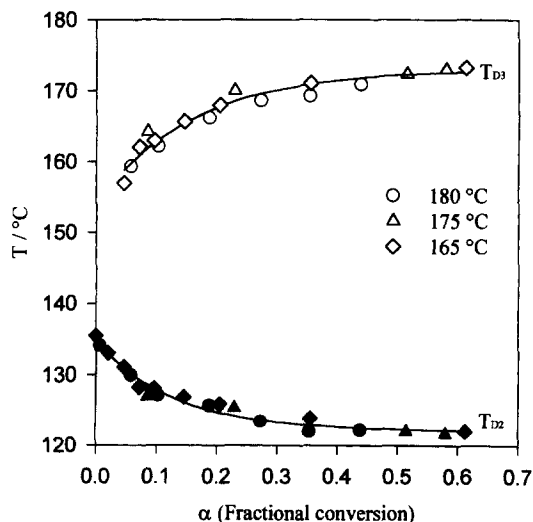


Figure 11 Changes of the transition temperature (T) of T_{D2} and T_{D3} as a function of fractional conversion for the Twin8e/SAA system processed at temperatures of 165, 175 and 180°C

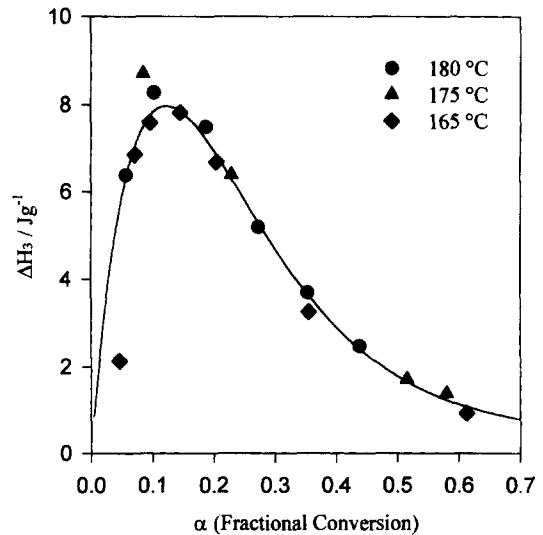


Figure 12 Changes of the transition enthalpy (ΔH) of T_{D3} as a function of fractional conversion for the Twin8e/SAA system processed at temperatures of 165, 175 and 180°C

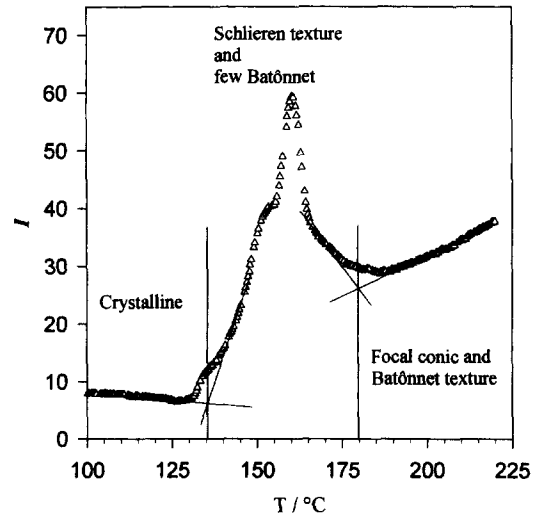


Figure 13 Changes in light scattering intensity (I) through crossed polarizers during a temperature scan from 100 to 220°C for the partially cured Twin 8e/SAA mixture. The sample was treated at 175°C for 3 min prior to the scan

isotropic. Thus, the second transition was a nematic–isotropic transition. However, above this transition, fine Batônnet textures with some focal conic component remained, and the light intensity from the textures stayed constant up to 220°C. These results mean that the Twin8e/SAA mixture itself displays a nematic phase whose clearing temperature is around 175°C, while the Twin8e–SAA adduct displayed a smectic phase whose clearing temperature was above 220°C. The precise clearing temperature of the smectic phase could not be measured because cross-linking occurred during heating. Previously, we believed that the smectic organization from the twin epoxy monomer was due to network formation which induced registration between the mesogenic groups. However, the Twin8e–SAA adduct formed a smectic phase prior to gelation. Since the sample had a low conversion of 0.1–0.2, there should be only dimers (Twin8e–SAA–Twin8e) or short oligomers in

the system. Strong interactions between sulfonamide groups may contribute to smectic order and result in an extremely high clearing temperature. It is thought the same scenario is likely for other LC epoxy monomer-SAA combinations such as the DOMS/SAA system.

The results of dynamic d.s.c. can be explained more precisely with the help of the POM results. As the monomers were reacted, the enthalpies of the nematic-isotropic transition decreased as the formation of the Twin8e-SAA adduct increased. The smaller endothermic peak located at 120°C (T_{D1}) may be attributed to the melting point of the Twin8e-SAA adduct, because a peak at T_{D1} increased as the reaction proceeded, whereas peaks at T_{D2} and T_{D3} became smaller.

X-ray diffraction studies of the Twin8e/SAA curing reaction

One of the best approaches to confirming smectic structure is using X-ray diffraction. Figure 14 shows a typical X-ray diffraction scan for the fully cured Twin8e/SAA mixture. The sharp diffraction peak at 44 Å and the broad peak around 4.3 Å are characteristic of a smectic structure. Table 3 shows X-ray diffraction data measured at room temperature for the Twin8e/SAA system cured at various temperatures. Values of correlation length (L)

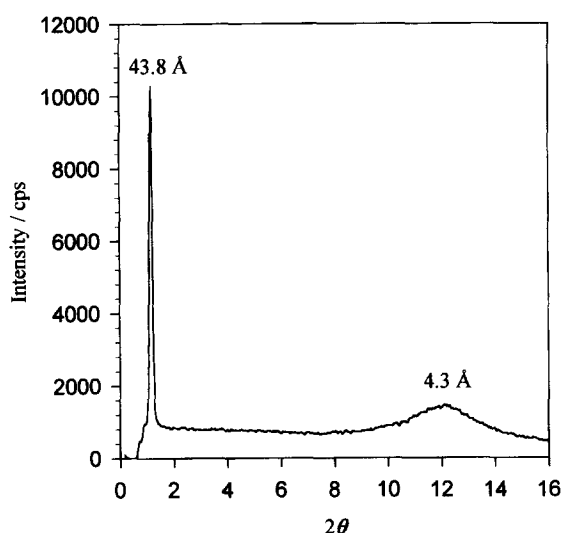


Figure 14 X-ray diffraction pattern measured at room temperature for the Twin8e/SAA system cured at 160°C for 3 h

were calculated using the Scherrer equation¹⁶:

$$L = \frac{K\lambda}{\beta_0 \cos \theta}$$

$$\beta_0 = 2\sqrt{w^2 - \left(\frac{0.2 \cos \theta}{\lambda \cos^2 2\theta}\right)^2} \quad (5)$$

$$K = 0.9$$

In equation (5), θ is the diffracted angle, λ is the wavelength of the monochromated X-ray beam, β_0 is the breadth of the reflection corrected for instrumental broadening, w is the full-width, half-maximum of the diffraction peak, and l is the distance between the sample and the detector. The intensity of the diffraction peak for the smectic layer spacing (I_s) was calculated from the integrated diffracted intensity of the entire peak area. For the Twin8e/SAA mixture, as the processing temperature was raised, the value of correlation length of both the smectic and the wide-angle diffraction peaks decreased, and the intensity of the smectic diffraction was also attenuated, indicating that curing at high temperatures produced more defective mesomorphic networks. These results are in good agreement with the observations from POM. Likewise, the curing temperature affected the d -spacing of both the smectic layer and the lateral distance between mesogenic groups.

Real-time X-ray diffraction measurements were carried out under the same conditions as the isothermal d.s.c. and POM experiments. Figure 15 displays growth of the smectic layer peak under various cure temperatures for the Twin8e/SAA system. The time when the smectic layer diffraction appeared (t_{x1}) and reached its maximum (T_{x2}) are displayed in Table 4. Also listed in Table 4 are the conversions α_{x1} and α_{x2} corresponding to t_{x1} and t_{x2} , respectively. The smectic layer diffraction appeared when conversion reached 0.20–0.30. Curing at low temperature tended to delay the formation of the smectic phase. In the discussion above concerning dynamic d.s.c. and POM results, we described the observation of a critical region around 175°C. From these results, we can infer that curing below 175°C forms a nematic phase prior to formation of the smectic phase.

Changes in correlation length and d -spacing were analysed for both the smectic layer and wide-angle diffraction. Figure 16 shows the results of smectic layer diffraction under isothermal conditions at 175°C. The d -spacing decreased from 47.0 to 42.7 Å as the curing reaction proceeded. This change is ascribed to

Table 3 Results of X-ray diffraction measured at room temperature for the Twin8e/SAA system cured at various temperatures

Cure temperature (°C)	Smectic layer diffraction			Wide-angle diffraction	
	d -spacing (Å)	L (Å)	Intensity (cps)	d -spacing (Å)	L (Å)
160	43.8	367.6	9853	4.30	23.3
165	44.4	379.0	7630	4.30	20.4
170	44.4	360.1	7478	4.30	18.3
175	44.4	337.0	7501	4.30	17.7
180	45.6	325.3	5781	4.32	17.0
185	45.6	294.3	3171	4.35	15.1
190	45.6	157.2	2574	4.41	14.9

polymerization shrinkage by the cross-linking reaction. The correlation length reached a maximum around 5 min after the smectic layer diffraction appeared, and then decreased. Similar behaviour was observed over the examined temperature range. Critical changes in both d -spacing and correlation length occurred at a fractional conversion of ~ 0.65 – 0.70 , and seem to be related to gelation. The value of 0.65 – 0.70 is somewhat higher than the theoretical gel point of 0.58 for the diepoxy and diamine stoichiometric mixture¹⁷. Changes in wide-angle diffraction could be observed (Figure 17). The change in lateral distance was only 1% while the smectic layer shrank 10%. This indicates that most of the cure shrinkage was concentrated along the longitudinal axis of the molecule. It is thought that an increase in the cross-link density is required to cause the observed changes in smectic order, which includes not only reduced smectic layer spacing but also the size of domains as well as the elastic curvature of molecules associated with disclinations. This change seems to be correlated with formation of a fine disclination structure in the optical texture and a reduction of the correlation length of the smectic layer. In contrast to the change in the smectic layer diffraction, the correlation length of the wide-angle diffraction increased slightly as the curing took place. The transition from the isotropic state to the LC state caused the increase. The intensity of the smectic layer diffraction continued to grow to a fractional

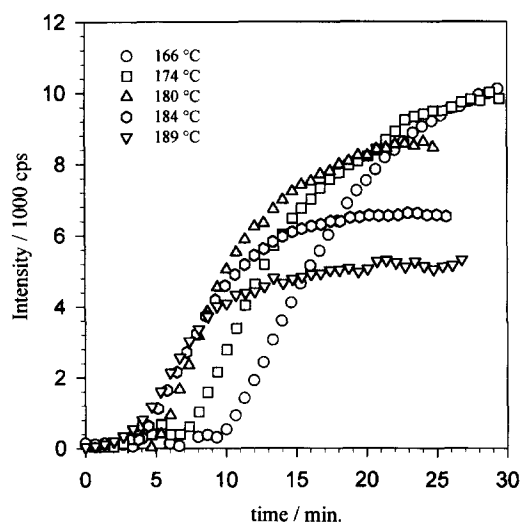


Figure 15 Evolution of the smectic layer diffraction intensity under isothermal cure temperatures of 166, 174, 180, 184 and 189°C for the Twin8e/SAA system

Table 4 Results of real-time X-ray diffraction studies of the Twin8e/SAA system cured under various isothermal conditions

Cure temperature (°C)	t_{x1} (min)	α_{x1}	t_{x2} (min)	α_{x2}
166	9.8	0.229	31	0.939
174	6.7	0.252	26	0.943
180	5.4	0.238	22	0.925
184	4.1	0.227	18	0.839
189	3.4	0.222	15	0.782

t_{x1} : time when smectic layer diffraction appeared. α_{x1} : corresponding fractional conversion to t_{x1}

t_{x2} : time when growth of smectic layer diffraction saturated. α_{x2} : corresponding fractional conversion to t_{x2}

conversion of 0.8 – 0.9 . This observation means that organization of the smectic layer occurred even in the gel state. Mormann *et al.* also reported that an isotropic–nematic transition occurred after the gel point in a dicyanate thermoset¹⁸.

Rheological studies of the Twin8e/SAA curing reaction

Rheological experiments were carried out under isothermal conditions (Figure 18). At a cure temperature between 165 and 175°C the evolution of thermoset viscosity was monitored. Parallel plates 25 mm in diameter were unable to detect the loss modulus accurately until the storage modulus reached the value around 500 Pa . A gel point where G' is equal to G'' was expected to be identified around the storage modulus of 10^4 – 10^5 Pa ¹⁹. However, a gel point could not be detected from these experiments, indicating that the Twin8e/SAA mixture behaved as an elastic fluid before gelation occurred. Chien *et al.*²⁰ reported a twin LC oligomer which showed unusually high elastic behaviour because

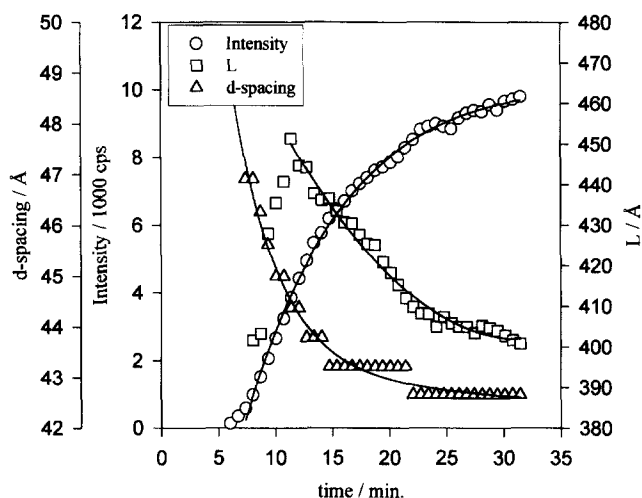


Figure 16 Changes of the diffraction intensity, the correlation length (L) and the d -spacing of smectic layer diffraction under isothermal cure at 174°C for the Twin8e/SAA system

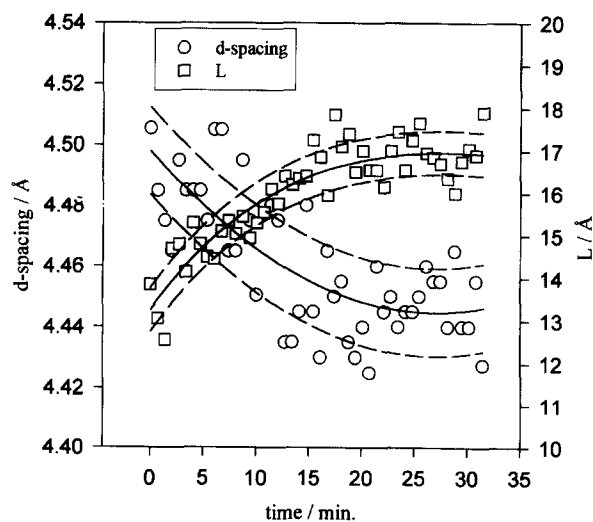


Figure 17 Changes of the correlation length (L) and the d -spacing of wide-angle diffraction under isothermal cure at 174°C for the Twin8e/SAA system

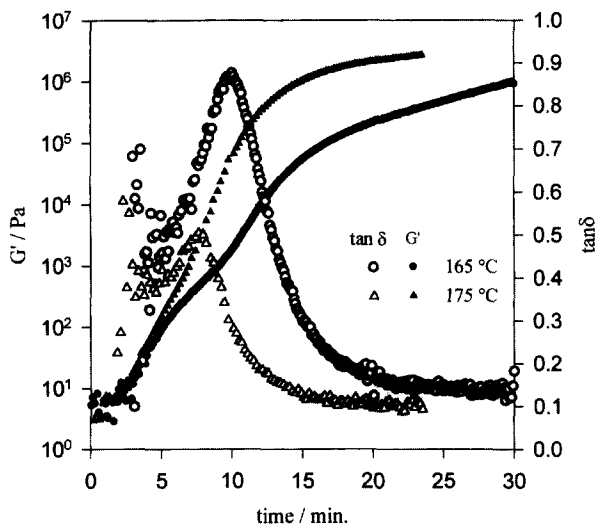


Figure 18 Evolution of the storage modulus (G') and changes of the loss tangent ($\tan \delta$) as a function of reaction time at 165 and 175°C for the Twin8e/SAA system

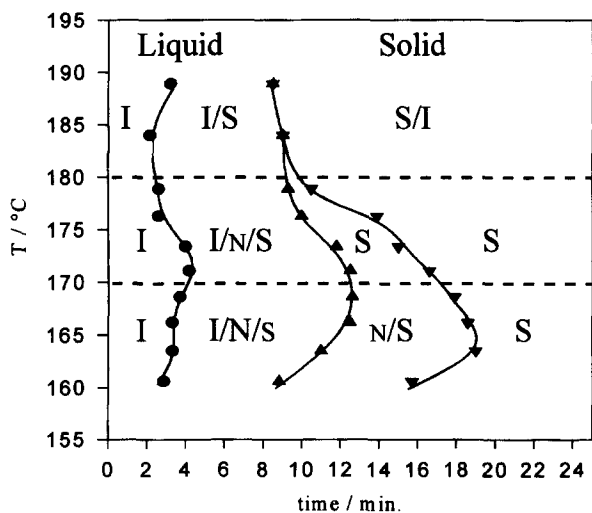


Figure 19 The TTT diagram under isothermal cure conditions for the Twin8e/SAA system. I, N and S denote isotropic, nematic and smectic, respectively

of physical cross-links present between the flexible spacers of the twin structure. Our observations may be explained in the same manner as those of Chien. A loss tangent maximum was detected at curing temperatures between 175 and 165°C. This transition is associated with a phase transition. A maximum for the loss tangent appeared at a fractional conversion of 0.28–0.32. This conversion is somewhat higher than that where the smectic layer diffraction appeared in the real-time X-ray diffraction measurement; however, a mechanical response requires larger amounts of smectic phase due to lower sensitivity. A conversion of 0.28–0.32 means that more than 50% of the twin epoxy monomers were converted to the Twin8e/SAA oligomers. We infer that the mechanical transition was due to formation of a smectic phase which leads to a slightly higher modulus and may also be associated with some reaction rate acceleration¹² in the smectic phase.

Time-temperature-phase transformation (TTT) diagram for the Twin8e/SAA system

The curing and phase behaviour of the Twin8e/SAA

system can be best summarized by the TTT diagram shown in Figure 19. The diagram shows a transition region which occurs in the curing temperature range between ~170 and 180°C. Above this region, a smectic phase forms directly from an isotropic melt whereas the smectic phase forms via a nematic phase below this temperature. Curing above this temperature regime results in a defective smectic structure characterized by dense disclination lines and low X-ray scattering from the smectic layer. It is a natural consequence for an LC thermoset that curing at high temperature produces a more defective structure due to an increase of thermal perturbation. The stimulated thermal motion of reactive sites favours the construction of disordered networks while anisotropic dispersion interactions and steric packing interactions act to retain the mesophase.

Curing at an intermediate temperature results in delayed formation of smectic order. This is due to the fact that the appearance of the LC state is a function of temperature, clearing temperature at some extent of polymerization, extent of polymerization, and rate of polymerization. These parameters are highly interrelated with each other. Due to the initial heterogeneity of the reactant mixture, the appearance time of an LC phase is less dependent upon the curing temperature.

CONCLUSION

Previously, we believed that formation of a smectic phase from the twin epoxy monomer was due to network formation which induced registration between mesogenic groups. This meant that cross-links were required to produce smectic organization. However, without any cross-links, the Twin8e/SAA oligomer produced a smectic phase which may be credited to strong interaction between the sulfonamide groups. Initial heterogeneity was a predominant factor in enabling an acceleration in curing rate. A large rate constant frequency factor in the mesophase was not the only factor for an acceleration in curing rate in the reaction of multicomponent thermosets such as the LC epoxy/diamine mixture. The cross-linking reaction caused fine disclination lines in the optical texture as well as a decrease of the smectic layer spacing. The smectic transition could be identified using POM experiments, real-time X-ray diffraction measurements and viscometric measurements. These three methods yielded slightly different values of the transition due to varying sensitivities, and only by combining these methods with d.s.c. studies could the nature of the smectic network formation be clarified.

ACKNOWLEDGEMENTS

The authors would like to thank Dr H. Körner for cooperation with the real-time X-ray experiments and valuable discussion of the results, Dr J. Navaie and the Cornell High Energy Synchrotron Source (CHESS) staff for their marvellous technical support during the CHESS experiments, Professor C. Cohen and his student J. Garcia for their assistance in connection with the rheological measurements, and the Cornell Materials Science Center for use of their computer facilities. This research was partially supported by Japan Synthetic Rubber Co., Ltd and the National Science Foundation.

REFERENCES

1. Barclay, G. G. and Ober, C. K., *Progr. Polym. Sci.*, 1993, **18**, 899.
2. Broer, D. J., Lub, J. and Mol, G. N., *Nature*, 1995, **378**, 467.
3. Mallon, J. J., Adams, P. M., *J. Polym. Sci. A: Polym. Chem.*, 1993, **31**, 2249.
4. Jahromi, S., *Macromolecules*, 1994, **27**, 2804.
5. Lin, Q., Yee, A. F., Earls, J. D., Hefner, R. E., Jr and Sue, H.-J., *Polymer*, 1994, **35**, 2679.
6. Robinson, A. A., McNamee, S. G., Freidzon, Y. S. and Ober, C. K., *Polym. Prepr. (Am. Chem. Soc., Div. Polym. Chem.)*, 1993, **34**(2), 743.
7. Shiota, A. and Ober, C. K., *J. Polym. Sci. A: Polym. Chem.*, 1996, **34**, 1291.
8. Stewart, J. J. P., *J. Computer-Aided Mol. Design*, 1990, **4**, 1.
9. Barton, J. M., *Adv. Polym. Sci.*, 1985, **72**, 112.
10. Hadad, D. K., in *Epoxy Resins*, 2nd edn, ed. C. A. May. Marcel Dekker, New York, 1988, Chap. 14, p. 1089.
11. Liu, J., Wang, C., Campbell, G. A., Earls, J. D. and Priester, R. D. Jr, *J. Polym. Sci. A: Polym. Chem.*, 1997, **35**, 1105.
12. Hoyle, C. E. and Watanabe, T., *Macromolecules*, 1994, **27**, 3790.
13. Douglas, E. P., Langlois, D. A. and Benicewicz, B. C., *Chem. Mater.*, 1994, **6**, 1925.
14. Amendola, E., Carfagna, C., Giamberini, M. and Pisaniello, G., *Macromol. Chem. Phys.*, 1995, **196**, 1577.
15. Mormann, W. and Bröcher, M., *Macromol. Chem. Phys.*, 1996, **197**, 1841.
16. Alexander, L. E., *X-Ray Diffraction Methods in Polymer Science*, reprint edn. Krieger, Huntington, NY, 1979.
17. Dusek, K., *Adv. Polym. Sci.*, 1986, **78**, 1.
18. Morman, W. and Zimmermann, J., *Macromol. Symp.*, 1995, **93**, 97.
19. Jahromi, S., Kuipers, W. A. G., Norder, B. and Mijs, W. J., *Macromolecules*, 1995, **28**, 2201.
20. Lin, Y. G., Zhou, R., Chien, J. C. W. and Winter, H. H., *Polymer*, 1989, **30**, 2204.